



Performance estimation of artificially roughened solar air heater duct provided with continuous ribs

Mridul Sharma, Varun

Department of Mechanical Engineering, National Institute of Technology, Hamirpur, 177005, India.

Abstract

The use of an artificial roughness on a surface is an effective technique to enhance the rate of heat transfer to fluid flow in the duct of a solar air heater. This paper presents a comparison of exergetic performance of solar air heaters having different types of geometry of roughness elements (continuous ribs) on the absorber plate. The exergy efficiency has been computed by using the correlations for heat transfer and friction factor developed by various investigators within the investigated range of operating and system parameters. The exergy efficiency (η_{Ex}) based criterion shows the better results at lower value of Re . There is not a single roughness geometry which gives best exergetic performance for whole range of Reynolds number. Solar air heater having rib-grooved and arc shaped wire as artificial roughness is found to have better exergy efficiency in the lower range of Reynolds number. However, smooth duct is found suitable in the higher range of Reynolds number.

Copyright © 2010 International Energy and Environment Foundation - All rights reserved.

Keywords: Artificial roughness, Continuous ribs, Exergy efficiency, Fluid flow, Solar air heaters.

1. Introduction

Solar air heaters, because of their inherent simplicity, are cheap and most widely used as collection devices of solar energy. Use of artificial roughness in the form of ribs on the absorber plate has been found to be an efficient method of enhancing the performance of solar air heater [1]. The thermal performance of conventional solar air heaters is generally poor because of the low convective heat transfer coefficient between the air and the absorber plate, leading to high absorber plate temperature and hence higher thermal losses. The low value of convective heat transfer coefficient is generally attributed to the presence of laminar sub-layer on the heat transferring surface. These ribs break the laminar boundary layer of turbulent flow and makes the flow turbulent adjacent to the wall and results in the desirable increase in the heat transfer. This also results in the undesirable increase in the pressure drop due to the increased friction. Hence, flow duct and absorber surface (ribs) of solar air heaters should be designed with the objectives of high heat transfer rates and low friction losses [2-4]. To balance useful energy and friction losses, second law considerations are suitable and exergy is a suitable quantity for the optimization of solar air heaters having different roughness elements on the absorber plate. Exergy is maximum work potential which can be obtained from energy [5-6]. Exergy analysis is an assessment technique for systems and processes that is based upon the second law of thermodynamics. Exergy analysis yields useful results because it deals with irreversibility minimization or maximum exergy delivery. The exergy analysis has been increasingly applied over the last several decades largely because of its advantages over energy analysis. Ozturk and Demirel [7] experimentally evaluated the energy and

exergy efficiencies of the thermal performance of a solar air heater having its flow channel packed with Raschig rings. Geng et al. [8] experimentally evaluated the exergy analysis of solar water heating system and compare the energy and exergy efficiencies. Kurtbas and Durmus [9] experimentally evaluated the energy efficiency, friction factor and dimensionless exergy loss of a solar air heater having five solar sub-collectors of same length and width arranged in series in a common case for various values of Reynolds number. In this paper, an exergy analysis has been done to carry out the performance evaluation of solar air heater having continuous rib as a roughness element on the absorber plate.

2. Literature review

The use of an artificial roughness on the underside of the absorber plate is an effective technique to enhance the rate of heat transfer to fluid flow in a solar air heater. The geometry of artificial roughness is to be such that it should break the laminar sub-layer for augmenting the heat transfer, and the core flow should not be unduly disturbed to limit the increase in friction losses. In case of solar air heaters, rib type roughness has been investigated mostly. The ribs can be continuous (full) or discrete (broken) depending on whether complete rib or the ribs in pieces are placed on the absorber plate. The shape of the rib can be rectangular, circular, wedge, chamfered and orientation of the ribs can be as transverse, inclined and V-shaped. Many investigators analyzed various roughness geometry and developed the correlations of the heat transfer coefficient and friction factor. Webb et al. [10] developed heat transfer and friction correlations for turbulent flow in tubes having repeated rib roughness. Han et al. [11] investigated the rib roughened surface for effects of rib shape, angle of attack, spacing and pitch to height ratio. They developed the correlation for friction factor and heat transfer. Prasad and Saini [3] investigated the effect of relative roughness height and relative roughness pitch on heat transfer and friction factor. They developed the relations to calculate the average friction factor and Stanton number for artificial roughness of absorber plate by small diameter protrusion wire. It has been observed that increase in the relative roughness height results in decrease of the rate of heat transfer enhancement although the rate of increase of friction factor increases. Increase in the relative roughness pitch results in a decrease in the rate of both heat transfer and friction factor. Gupta et al. [12] investigated the effect of relative roughness height, angle of attack and Reynolds number on heat transfer and friction factor in rectangular duct having circular wire ribs on the absorber plate. The correlations were developed for Nusselt number and friction factor in terms of system and operating parameters. They found that the maximum heat transfer coefficient and friction factor were found at an angle of attack 60° and 70° in the range of parameters investigated. They also carried out the thermo-hydraulic performance in terms of effective efficiency of solar air heater with rib roughened surface by using heat transfer and friction factor correlation developed by them. Saini and Saini [13] investigated the effect of expanded metal mesh geometry as artificial roughness, and developed the correlations for Nusselt number and friction factor. The effect of expanded metal mesh geometry on the heat transfer coefficient and friction factor has been investigated. Verma and Prasad [14] developed the heat transfer and friction factor correlation for roughness elements consisting of small diameter wires, and evaluated the thermo-hydraulic performance. Bhagoria et al. [4] performed experiments to determine the effect of relative roughness pitch, relative roughness height and wedge angle on the heat transfer and friction factor in a solar air heater roughened duct having wedge shaped rib roughness. The presence of ribs yields Nusselt number up to 2.4 times while the friction factor rises up to 5.3 times as compared to smooth duct in the range of parameters investigated. A maximum enhancement in heat transfer was obtained at a wedge angle of about 10° . The heat transfer was found maximum for a relative roughness pitch of about 7.57. Jaurker et al. [15] experimentally investigated the heat transfer and friction factor characteristics of rib-grooved artificial roughness on one broad wall. They carried out the thermo-hydraulic performance analysis of air duct and concluded that rib-grooved arrangement is better than rib only. The effect of relative roughness pitch, relative roughness height and relative groove position on the heat transfer coefficient and friction factor studied. They found that the maximum heat transfer was obtained for a relative roughness pitch of about 6. The optimum condition for heat transfer was found at a groove position to pitch ratio of 0.4. Saini and Saini [16] developed the correlations for Nusselt number and friction factor having arc shaped wire type roughness on the absorber plate. They found that there is considerable enhancement in heat transfer coefficient is achieved by providing arc-shape parallel geometry as artificial roughness with solar air heater duct. The maximum enhancement in Nusselt number has been obtained as 3.80 times corresponding the relative arc angle of 0.3333 at relative roughness height of 0.0422. However, the increment in friction factor corresponding to these parameters has been observed 1.75 times only. Varun et al. [17] developed the correlations for Nusselt number and

friction factor for roughness elements consisting of combination of inclined as well as transverse ribs on the absorber plate and evaluated the thermal performance. The experimental investigation encompassed the Reynolds number ranges from 2000 to 14,000, relative roughness pitch as 3-8 and relative roughness height of 0.03. The effects of these parameters on the heat transfer coefficient and friction factor were discussed. Similar investigations for heat transfer and fluid flow characteristics have been carried out by Karwa et al. [18] for chamfered rib; Momin et al. [19] for V-Shaped rib; Muluwork et al. [20] for V-Shaped staggered discrete rib; Layek et al. [21] for chamfered rib-groove roughness. Mittal et al. [22] evaluated and compared the effective efficiency of solar air heaters having different roughness geometry on absorber plate, for a fixed set of parameters. They plotted the variation of effective efficiency with Reynolds number for smooth absorber plate, as well as roughened absorber plate solar air heaters for different relative roughness height. It is evident that various investigators have developed correlations for heat transfer and friction factor for solar air heater ducts having artificial roughness of different geometries. Several researchers carried out the effective efficiency evaluation, but the exergy based performance evaluation of solar air heater duct having continuous ribs as artificial roughness on absorber plate has not been reported so far.

3. Modeling of solar air heater

The exergetic performance analysis for various continuous ribs on the absorber plate has been carried out. The schematic diagram of the ribs has been shown in Figure 1. The collector under consideration consists of a flat glass cover, an absorber plate which is artificially roughened and a well insulated parallel bottom plate forming a passage through which the air to be heated flows. The rate of useful thermal energy may be obtained from the equation [12]:

$$Q_u = F' [I(\tau\alpha) - U_L(T_o - T_i)/2] A_p \quad (1)$$

where Q_u is the useful heat gain (W), F' is the collector efficiency factor, I is the irradiance (W.m^{-2}), $(\tau\alpha)$ is the transmittance-absorptance product for absorber cover combination, U_L is the overall loss coefficient ($\text{W.m}^{-2}.\text{K}^{-1}$), A_p is the area of absorber plate (m^2), T is the temperature (K) and the subscripts (i) and (o) are the inlet and outlet respectively.

$$F' = [h/(h + U_L)] \quad (2)$$

where h is the convective heat transfer coefficient ($\text{W.m}^{-2}.\text{K}^{-1}$).

The rate of useful thermal energy gain in a roughened solar air heater may also be calculated from the following equations:

$$Q_u = hA_p(T_{pm} - T_{fm}) \quad (3)$$

where T is the temperature (K) and the subscripts (pm) and (fm) are the mean plate and mean fluid respectively.

$$Q_u = mc_p(T_o - T_i) \quad (4)$$

where m is the mass flow rate (kg.s^{-1}), c_p is the heat capacity of the fluid ($\text{kJ.kg}^{-1}.\text{K}^{-1}$).

Considering solar air heater (Figure 2) as a control volume, the law of exergy balance [5] for this control volume can be written as:

$$Ex_i + Ex_{c,s} + Ex_w = Ex_o + IR \quad (5)$$

where Ex_i is exergy associated with mass flow of collector fluid entering the control volume (J.s^{-1}); Ex_o is exergy associated with mass flow rate leaving the control volume (J.s^{-1}); $Ex_{c,s} = IA_p\psi$ [23] is exergy of solar radiation falling on glass cover (J.s^{-1}), where ψ is the energy to exergy ratio for radiation; Ex_w is exergy of work input required to pump the fluid through air heater (J.s^{-1}), and IR is irreversibility or exergy destruction of the process.

$$IR = Ex_{c,s} - (Ex_o - Ex_i - Ex_w) \quad (6)$$

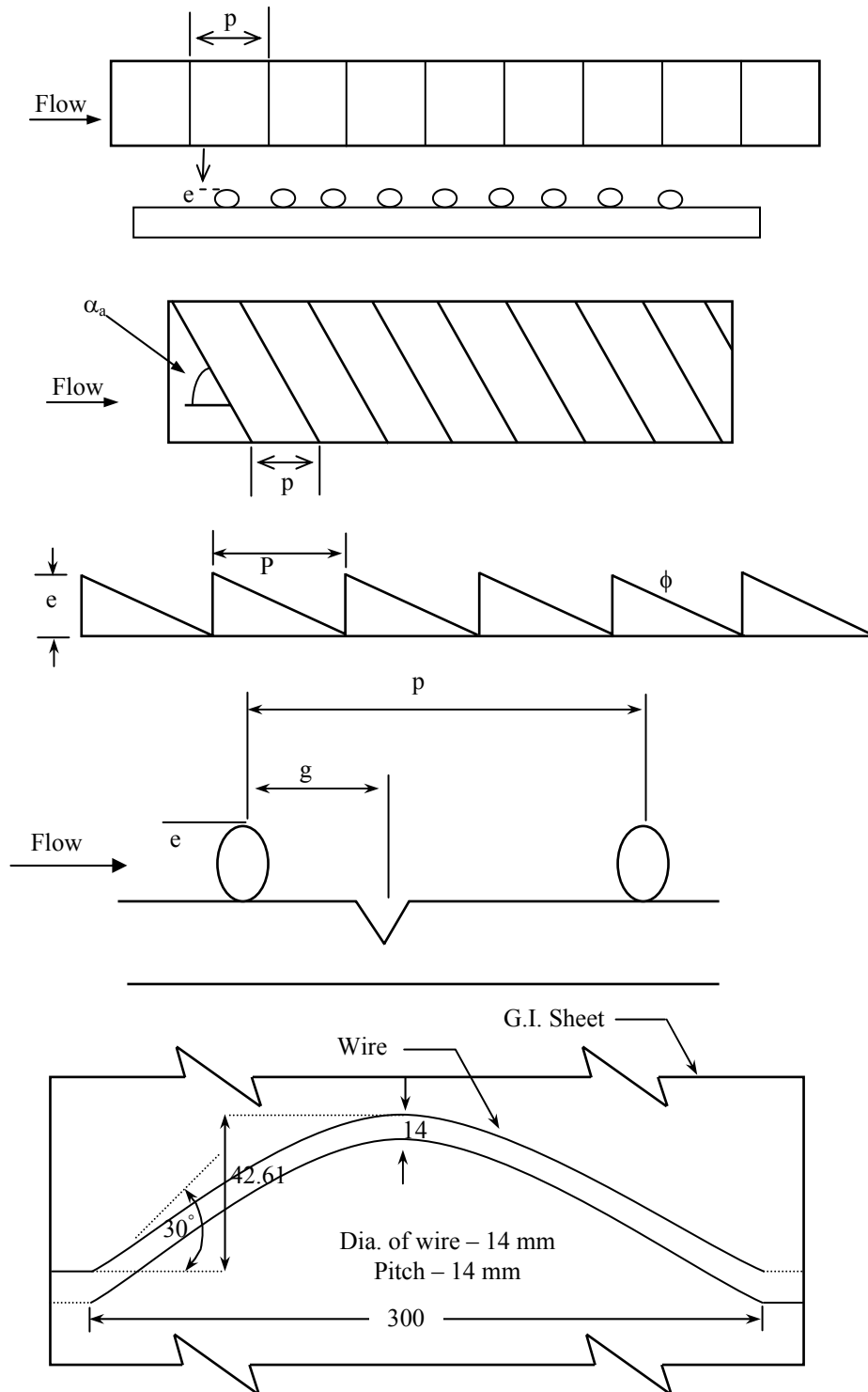


Figure 1. Roughness geometries: (a) small diameter protrusion wire [3], (b) angled circular rib [12], (c) wedge shaped rib [4], (d) rib-grooved [15], (e) arc shaped wire [16]

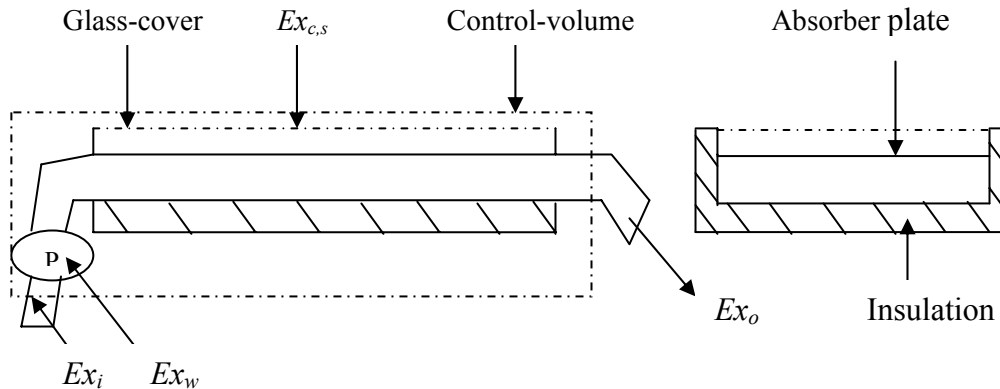


Figure 2. Flat plate solar air heater

The term in the bracket in Equation 6 represents the useful exergy or exergy output rate delivered by the solar collector. As the exergy of solar radiation falling on glass cover is fixed for a particular instant; thus minimization of irreversibility is equivalent to maximization of exergy output rate delivery of collector. For an incompressible fluid or perfect gas, the exergy or exergy output rate ' Ex_u ' ($J.s^{-1}$) delivered by a solar collector can be written as:

$$Ex_u = mc_p [(T_o - T_i) - T_a \ln(T_o / T_i)] = Q_u - mc_p T_a \ln(T_o / T_i) \quad (7)$$

where T_a is the ambient temperature (K).

The $Ex_{u,p}$, actual exergy rate delivered ($J.s^{-1}$) considering pressure drop of collector fluid is:

$$Ex_{u,p} = Ex_u - Ex_{d,p} \quad (8)$$

where the exergy destruction due to pressure drop $Ex_{d,p}$ ($J.s^{-1}$) is:

$$Ex_{d,p} = (T_a / T_i) W_p \quad (9)$$

where W_p is the pump work (W);

$$W_p = m \Delta p / \eta_{pm} \rho \quad (10)$$

where Δp is the pressure drop across collector length ($N.m^{-2}$), η_{pm} is the pump-motor efficiency ($= 0.85$), and ρ is the density of air ($kg.m^{-3}$).

The pressure loss Δp through air heater duct is:

$$\Delta p = (2fLV^2\rho) / d \quad (11)$$

where f is the friction factor, L is the collector length (m), V is the velocity of air in solar air heater duct ($m.s^{-1}$), and d is the equivalent diameter of air passage (m);

$$d = 2WH / (W + H) \quad (12)$$

where W is the collector width (m), and H is the solar air heater duct depth (m).

The values of heat transfer coefficient, h and friction factor, f for roughened and smooth solar air heaters have been determined from the correlations developed for heat transfer and friction factor by several investigators as given in Table 1.

The exergy efficiency of solar air heater based on second law of thermodynamics, by taking exergy of sun radiation [23], can be written as:

$$\eta_{Ex} = Ex_{u,p} / A_p I \psi = Ex_{u,p} / A_p I [1 - 4/3(T_a / T_s) + 1/3(T_a / T_s)^4] \quad (13)$$

4. Numerical calculations

Numerical calculations have been carried out to evaluate the exergy efficiency for a collector configuration, system properties and operating parameters. The selected environmental and design conditions of the solar air heater and constant parameters considered under the present investigation are as given in Table 2. The heat gain and outlet temperature of air are calculated by using Equations 1, 2 and 4. The exergy output rate is calculated using Equations 7-12. The exergy efficiency is evaluated from Equation 13. The performance evaluation has been carried out for various values of relative roughness height (e/d), irradiance (I) and overall heat loss coefficient (U_L).

5. Results and discussion

The exergy efficiency of roughened as well as smooth absorber plate solar air heaters has been computed on the basis of second law of thermodynamics, by taking exergy of sun radiation [23]. For exergy efficiency of solar air heater, the relative roughness height (e/d) is considered as strong parameter of roughness element. Figures 3-10 have been prepared to show the effect of relative roughness height, irradiance and overall heat loss coefficient on exergy efficiency for the optimal values of other parameters suggested by various investigators. It can be observed from these Figures that for given values of roughness parameters, similar trend in variation of exergy efficiency is obtained with Reynolds number. The exergy efficiency decreases with Reynolds number and for higher values of Reynolds number it approaches zero, even becomes negative. This is due to the fact that the quality of collected heat decreases and pump work increases. It is also observed that exergy efficiency corresponding to higher values of roughness height is better in lower range of Reynolds number; however value of exergy efficiency is reversed in higher range of Reynolds number. This effect can be attributed to the fact that at lower Reynolds number, the increase in the friction losses in the duct is insignificant with increase in relative roughness height, while the increase in heat transfer from roughened surface is quite substantial due to increase of turbulence in the vicinity of roughened surface. Figures 3-6 shows the variation of exergy efficiency (η_{Ex}) with Re , for various considered geometries. It is evident that exergy efficiency (η_{Ex}) decreases as the Re increases. It is observed that at lower value of Re ($=8000$), rib-grooved ribs shows the better exergy efficiency. Then, up to $12000 Re$, arc shaped wire as roughness element results in better exergetic performance. However, in higher range of Re (beyond 12000) the performance of smooth air heater is seen to be better than that of a roughened solar air heaters. The reason for this is that at higher Re the $Ex_{d,p}$ approaches Ex_u due to increase in pumping power requirement. Figures 3 and 5 and Figures 4 and 6 shows the effect of irradiance (I) on exergy efficiency for a given relative roughness height and Reynolds number. These Figures show that the exergy efficiency of solar air heaters is high at higher value of irradiance (I). It is also observed from the Figures that with increment in overall heat loss coefficient (U_L), the exergy efficiency decreases. Figures 7-10 shows the variation of exergy efficiency (η_{Ex}) with Re for increased value of relative roughness height (e/d). It is observed from these Figures that at low Re (less than 12000), the exergy efficiency increases with increment in e/d . However, it starts decreasing rapidly at higher Re (beyond 12000). This is due to the fact that the rate of useful energy collected decreases, whereas the friction losses rise with increasing relative roughness height causing increased energy consumption. The effect of irradiance and overall heat loss coefficient is similar as discussed before (Figures 3-6). The exergy efficiency (η_{Ex}) also follows the trend, of variation among various considered geometries, as indicated by Figures 3-6. For lower range of Re (up to 8000), rib-grooved ribs show better exergetic performance as compared to other geometries. For moderate value of Re (up to 12000), arc shaped wire as roughness element results in better exergy efficiency. Then, beyond $12000 Re$ value, smooth air heater is seen to be better than that of a roughened solar air heaters. But the trend of variation among various considered geometries is changed at higher value of Re . At higher Re , the η_{Ex} in general increases in the following sequence: small diameter protrusion wire, wedge shaped rib, rib-grooved, angled circular rib, arc shaped wire, smooth duct.

Table 1. Correlations developed for heat transfer coefficient and friction factor for different roughness geometries used in solar air heater duct

Authors	Type of roughness	Range of parameters	Heat transfer coefficient	Correlations	Friction factor
Prasad and Saini [3]	Small diameter protrusion wire	e/d: 0.02-0.033 p/e: 10-20 Re: 5000-50,000	$\bar{St} = \frac{\bar{f}/2}{1 + \sqrt{\bar{f}/2} \{4.5(e^+)^{0.57} - 0.95(p/e)^{0.53}\}}$		$\bar{f} = \frac{(W + 2B)f_s + Wf_r}{2(W + B)}$ Where $f_r = \frac{[0.95(p/e)^{0.53} + 2.5 \ln(d/2e) - 3.75]^2}{2}$
Gupta et al. [12]	Angled circular rib	e/d: 0.020-0.053 p/e: 7.5 & 10 α_a : 30°-90° Re: 5000-30,000	$Nu_r = 0.0024(e/d)^{0.001} (W/H)^{-0.06} Re^{1.084} \exp[-0.04(1 - \alpha_a / 60)^2]$ $Nu_r = 0.0071(e/d)^{-0.24} (W/H)^{-0.028} Re^{0.88} \exp[-0.475(1 - \alpha_a / 60)^2]$	for $e^+ < 35$ for $e^+ > 35$	$f_r = 0.1911(e/d)^{0.196} (W/H)^{-0.093} Re^{-0.165} \exp[-0.993(1 - \alpha_a / 70)^2]$
Bhagoria et al. [4]	Wedge-shaped rib	e/d: 0.015-0.033 p/e: 60.17 $\phi^{-1.0264} <$ p/e < 12.12 ϕ : 8, 10, 12, 15 Re: 3000-18,000	$Nu_r = 1.89 \times 10^{-4} Re^{1.21} (e/d)^{0.426} (p/e)^{2.94} \exp[-0.71\{\ln(p/e)\}^2 (\phi/10)^{-0.018} \times \exp[-1.5\{\ln(\phi/10)\}^2]]$		$f_r = 12.44 Re^{-0.18} (e/d)^{0.99} (p/e)^{-0.52} (\phi/10)^{0.49}$
Jaurker et al. [15]	Rib-grooved	e/d: 0.0181-0.0363 p/e: 4.5-10 Re: 3000-21,000 g/p: 0.3-0.7	$Nu_r = 0.002062 Re^{0.956} (e/d)^{0.349} (p/e)^{3.218} \times \exp[-0.868\{\ln(p/e)\}^2] (g/p)^{1.108} \times \exp[2.486 \times \{\ln(g/p)^2 + 1.406\{\ln(g/p)^3\}]$		$f_r = 0.001227 Re^{-0.199} (e/d)^{0.585} (p/e)^{7.19} \exp[-1.854\{\ln(p/e)\}^2] \times (g/p)^{0.645} \times \exp[1.513\{\ln(g/p)^2 + 0.8662\{\ln(g/p)^3\}]$
Saini and Saini [16]	Arc shaped wire	e/d: 0.0213-0.0422 p/e: 10 W/H: 12 α_a : 90-0.3333-0.6666 Re: 2000-17,000	$Nu_r = 0.001047 Re^{1.3186} (e/d)^{0.3772} (\alpha_a / 90)^{-0.1198}$		$f_r = 0.14408 Re^{-0.17103} (e/d)^{0.1765} (\alpha_a / 90)^{0.1185}$
Dittus-Boelter and Blasius	Smooth duct	-	$h_s = 0.024(k/d) \times Re^{0.8} \times Pr^{0.4}$		$f_s = 0.085 \times Re^{-0.25}$

where (e/d) is the relative roughness height, (p/e) is the relative roughness pitch, (Re) is the Reynolds number, (S_r) is the average Stanton number, (S_r) is the average friction factor, (W) is the collector width (m), (B) is the solar air heater duct height (m), (e^+) is the roughness Reynolds number [$= (e/d) \times (f/2) \times (Re)$], (Pr) is the Prandtl number, (f) is the friction factor, (Nu) is the Nusselt number, (α_a) is the angle of attack of roughness elements (°), (W/H) is the duct aspect ratio, ϕ is the wedge angle (°), (g/p) is the relative groove position, (h) is the convective heat transfer coefficient (W.m⁻².K⁻¹), (k) is the thermal conductivity of air (W.m⁻¹.K⁻¹), (d) is the equivalent diameter of passage (m). The subscripts (s) and (r) are the rough and smooth respectively.

Table 2. Typical values of system and operating parameters

Collector parameters	Values
Length , L (mm)	1000
Width , W (mm)	200
Height , H (mm)	20
Irradiance , I (W.m^{-2})	800-1000
Overall loss coefficient , U_L ($\text{W.m}^{-2}.\text{K}^{-1}$)	5-10
Transmittance-absorbance , ($\tau\alpha$)	0.85
Average inlet temperature of air , T_i (K)	298
Relative roughness height , e/d	0.02-0.04
Relative roughness pitch, p/e	10
Reynolds number , Re	2000-22,000

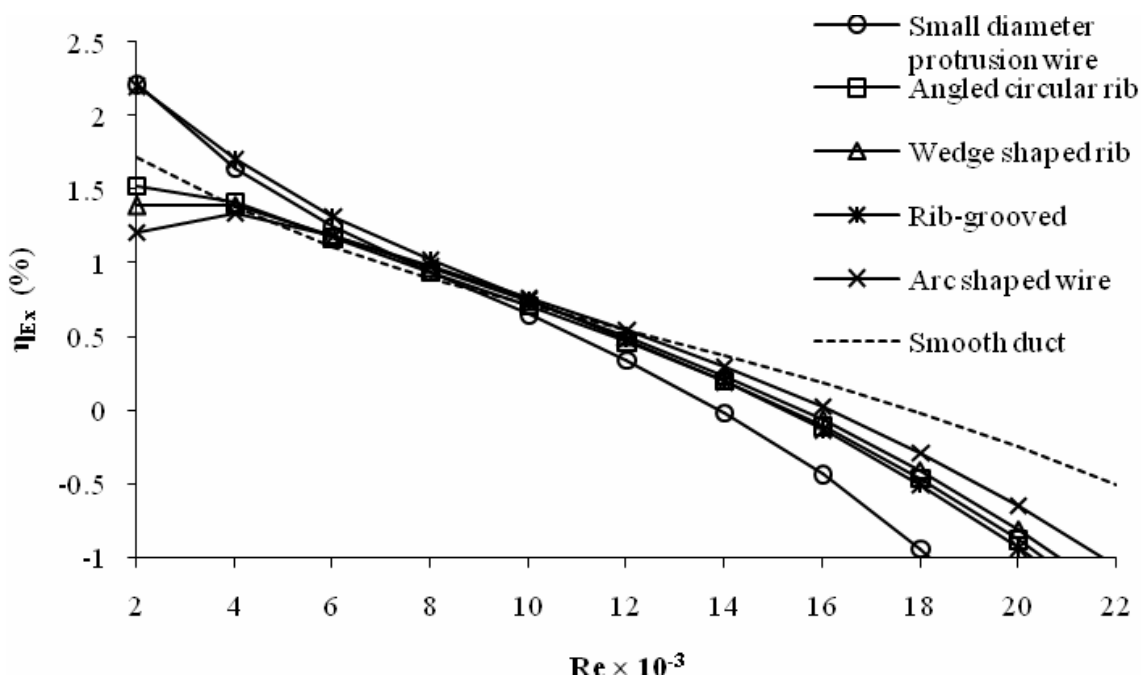


Figure 3. Variation of exergy efficiency with Reynolds number for various roughness geometries (at $e/d=0.02$, $I=1000 \text{ W/m}^2$ and $U_L=5 \text{ W/m}^2\text{-K}$)

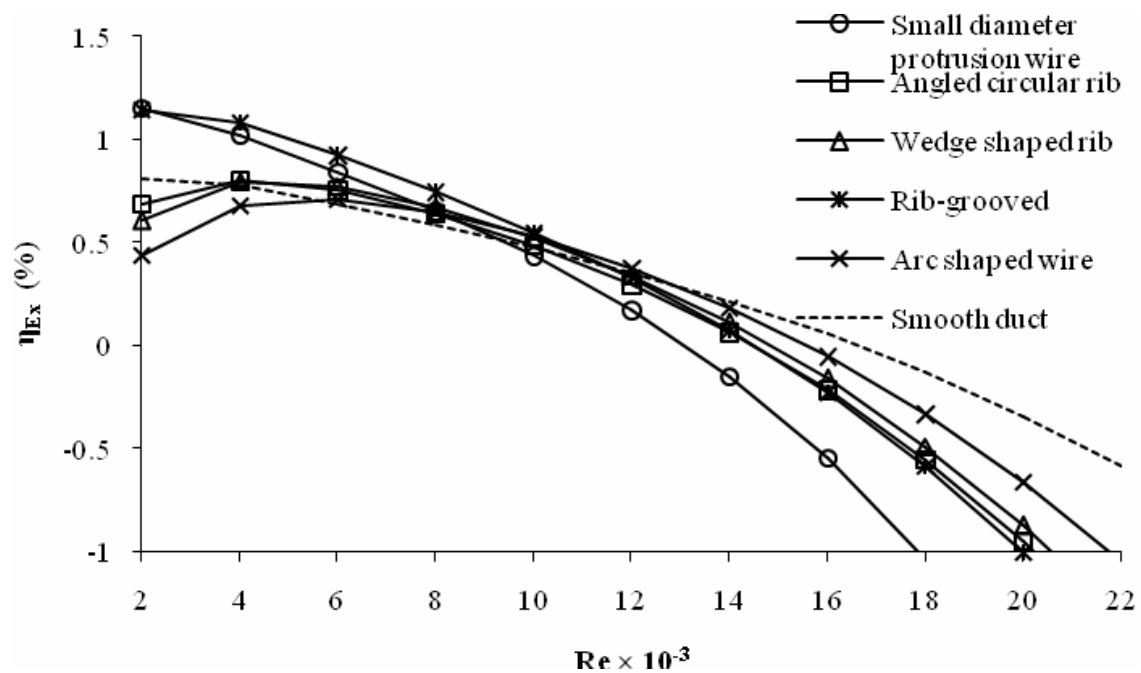


Figure 4. Variation of exergy efficiency with Reynolds number for various roughness geometries (at $e/d = 0.02$, $I = 1000 \text{ W/m}^2$ and $U_L = 10 \text{ W/m}^2\text{-K}$)

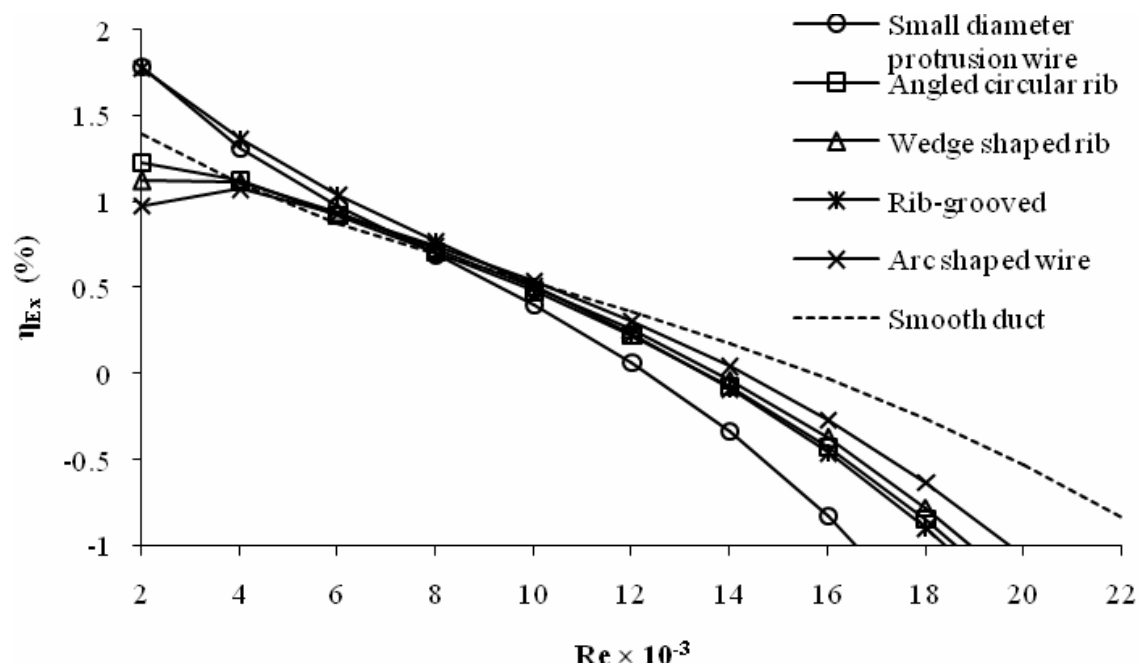


Figure 5. Variation of exergy efficiency with Reynolds number for various roughness geometries (at $e/d = 0.02$, $I = 800 \text{ W/m}^2$ and $U_L = 5 \text{ W/m}^2\text{-K}$)

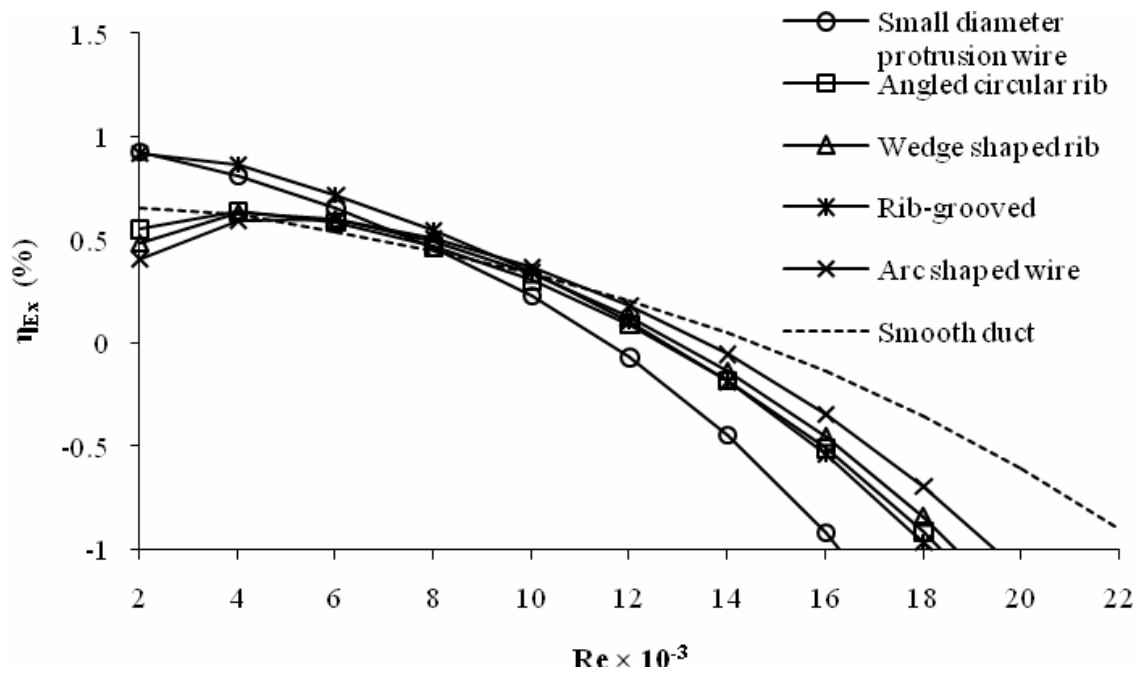


Figure 6. Variation of exergy efficiency with Reynolds number for various roughness geometries (at $e/d = 0.02$, $I = 800 \text{ W/m}^2$ and $U_L = 10 \text{ W/m}^2\text{-K}$)

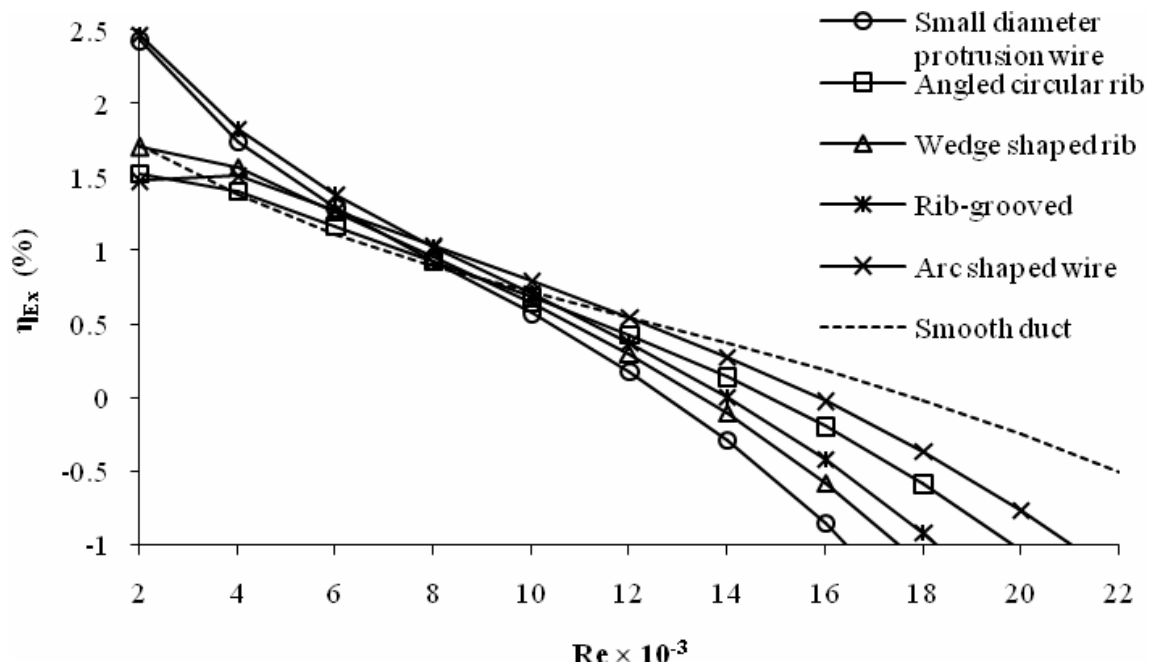


Figure 7. Variation of exergy efficiency with Reynolds number for various roughness geometries (at $e/d = 0.035$, $I = 1000 \text{ W/m}^2$ and $U_L = 5 \text{ W/m}^2\text{-K}$)

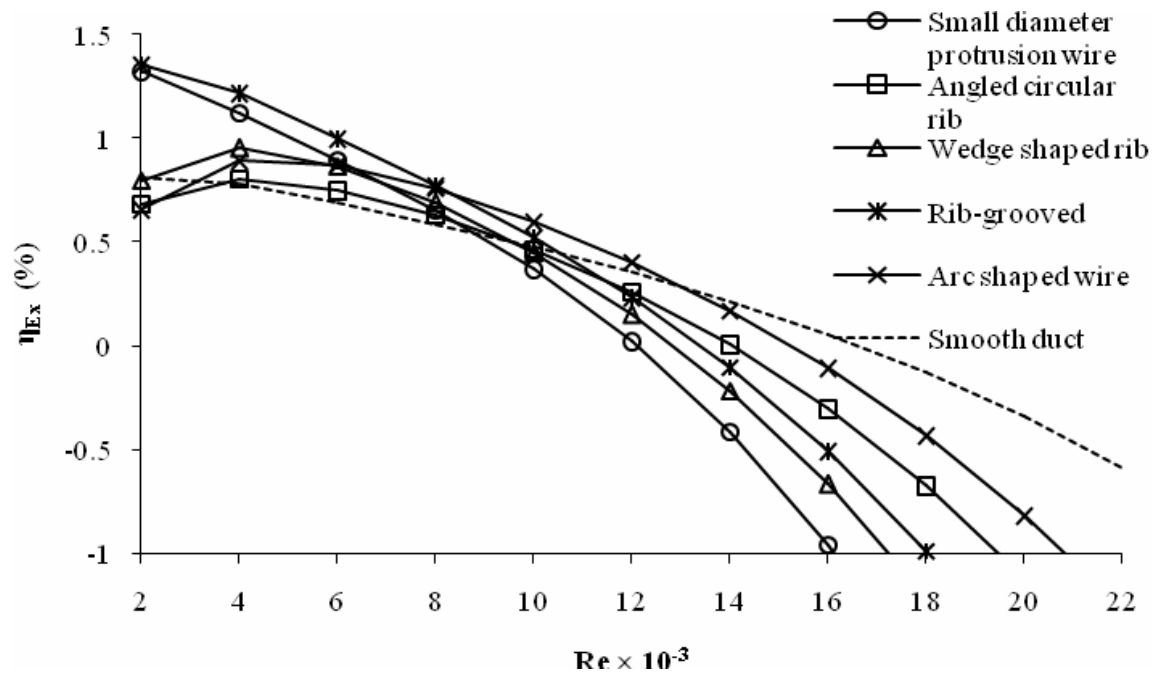


Figure 8. Variation of exergy efficiency with Reynolds number for various roughness geometries (at $e/d = 0.035$, $I = 1000 \text{ W/m}^2$ and $U_L = 10 \text{ W/m}^2\text{-K}$)

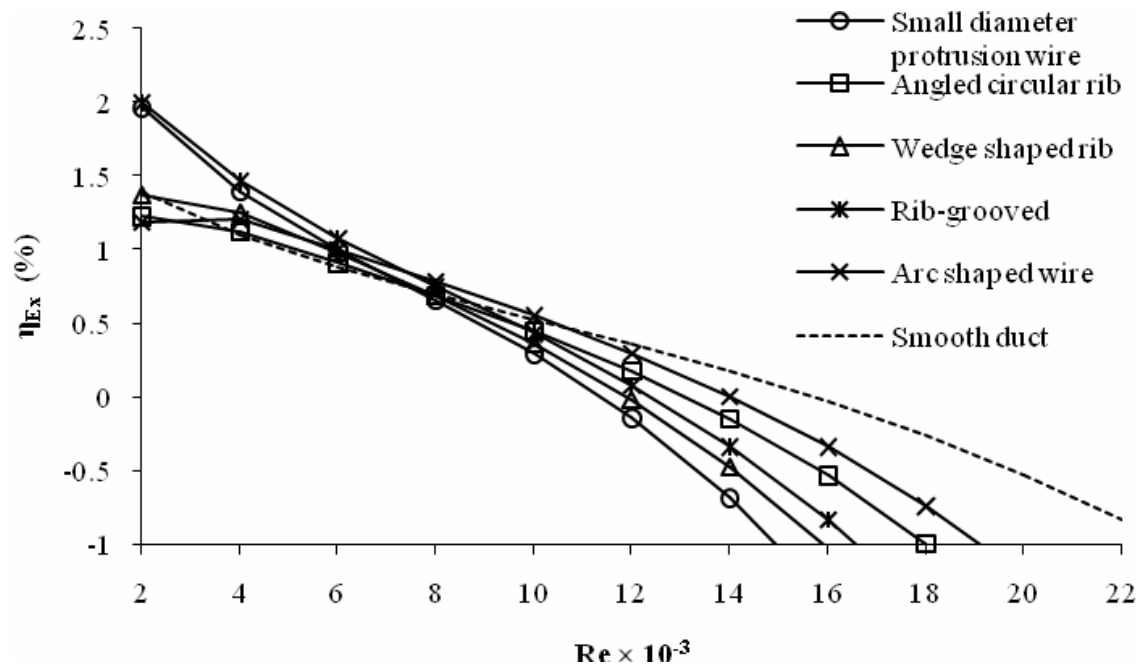


Figure 9. Variation of exergy efficiency with Reynolds number for various roughness geometries (at $e/d = 0.035$, $I = 800 \text{ W/m}^2$ and $U_L = 5 \text{ W/m}^2\text{-K}$)

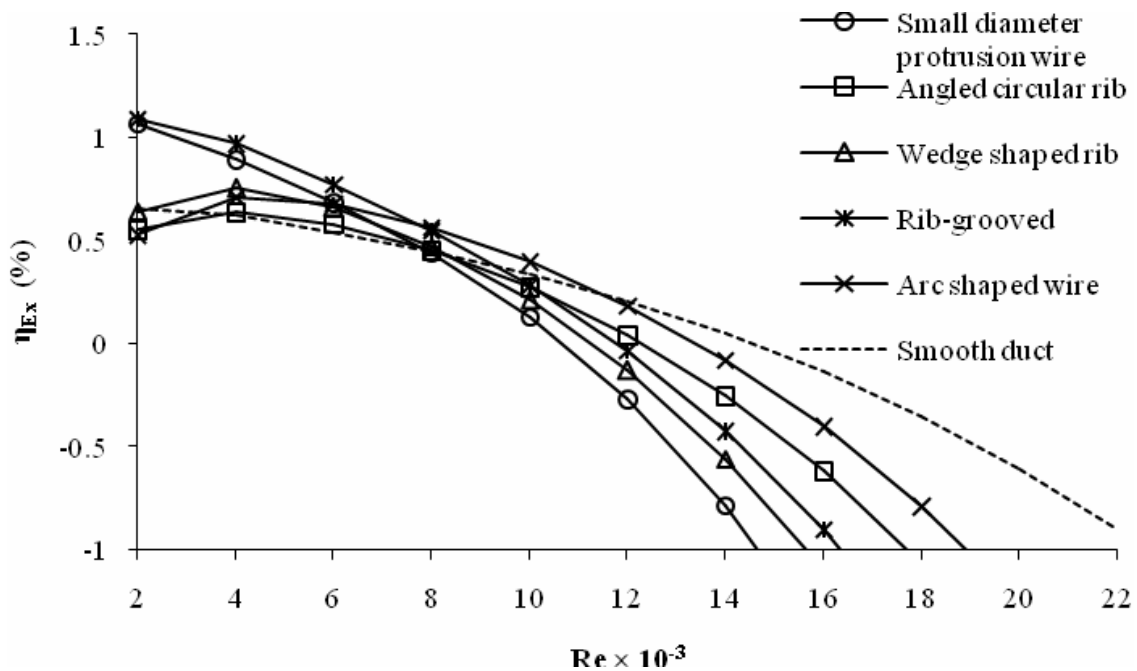


Figure 10. Variation of exergy efficiency with Reynolds number for various roughness geometries (at $e/d = 0.035$, $I = 800 \text{ W/m}^2$ and $U_L = 10 \text{ W/m}^2\text{-K}$)

8. Conclusion

The exergy efficiency is improved by using roughened geometries in the duct of solar air heater. The exergy efficiency (η_{Ex}) based criterion shows the better results at lower value of Re , at higher value of Re , the exergy efficiency becomes negative or exergy of pump work required exceeds the exergy of collected heat energy by solar air heater. Exergy analysis yields useful results and provides meaningful criterion for performance evaluation. There is not a single roughness geometry which gives best exergetic performance for whole range of Reynolds number. Solar air heater having rib-grooved and arc shaped wire as artificial roughness is found to have better exergy efficiency in the lower range of Reynolds number. However, smooth duct is found suitable in the higher range of Reynolds number.

References

- [1] Varun, Saini R.P., Singal S.K. A review on roughness geometry used in solar air heaters. *Solar Energy*. 2007, 81(11), 1340-1350.
- [2] Prasad K., Mullick S.C. Heat transfer characteristics of a solar air heater used for drying purpose. *Applied Energy*. 1985, 12(2), 83-93.
- [3] Prasad B., Saini J.S. Effect of artificial roughness on heat transfer and friction factor in a solar air heater. *Solar Energy*. 1988, 41(6), 555-560.
- [4] Bhagoria J.L., Saini J.S., Solanki S.C. Heat transfer coefficient and friction factor correlations for rectangular solar air heater duct having transverse wedge shaped rib roughness on the absorber plate. *Renewable Energy*. 2002, 25(3), 341-369.
- [5] Bejan A. *Advanced engineering thermodynamics*. Wiley Interscience Publishers, 1988.
- [6] Cengel Y.A., Boles M.A. *Thermodynamics: An Engineering Approach*. Tata McGraw Hill, 5th Edn, 2006.
- [7] Ozturk H.H., Demirel Y. Exergy based performance analysis of packed bed solar air heaters. *International J. of Energy Research*. 2004, 28(21-22), 423-432.
- [8] Geng L., Cengel Y.A., Turner R.H. Exergy analysis of a solar heating system. *J. of Solar Energy Engineering*. 1995, 117(3), 249-251.
- [9] Kurtbas I., Durmus A. Efficiency and exergy analysis of a new solar air heater. *Renewable Energy*. 2004, 29(9), 1489-1501.
- [10] Webb R.L., Eckert E.R.G., Goldstein, R.J. Heat transfer and friction in tubes with repeated rib roughness. *International J. of Heat and Mass Transfer*. 1971, 14(4), 601-617.

- [11] Han J.C., Zhang Y.M. High performance heat transfer ducts with parallel, broken and V-shaped broken ribs. *International J. of Heat and Mass Transfer*. 1992, 35(2), 513-523.
- [12] Gupta D., Solanki S.C., Saini J.S. Thermohydraulic performance of solar air heaters with roughened absorber plates. *Solar Energy*. 1997, 61(1), 33-42.
- [13] Saini R.P., Saini J.S. Heat transfer and friction factor correlations for artificially roughened ducts with expanded metal mesh as roughened element. *International J. of Heat and Mass Transfer*. 1997, 40(4), 973-986.
- [14] Verma S.K., Prasad B.N. Investigation for the optimal thermohydraulic performance of artificially roughened solar air heaters. *Renewable Energy*. 2000, 20(1), 19-36.
- [15] Jaurker A.R., Saini J.S., Gandhi B.K. Heat transfer coefficient and friction characteristics of rectangular solar air heater duct using rib-grooved artificial roughness. *Solar Energy*. 2006, 80(8), 895-907.
- [16] Saini S.K., Saini R.P. Development of correlations for Nusselt number and friction factor for solar air heater with roughened duct having arc-shaped wire as artificial roughness. *Solar Energy*. 2008, 82(12), 1118-1130.
- [17] Varun, Saini R.P., Singal S.K. Investigation of thermal performance of solar air heater having roughness elements as a combination of inclined and transverse ribs on the absorber plate. *Renewable Energy*. 2008, 33(6), 1398-1405.
- [18] Karwa R., Solanki S.C., Saini J.S. Heat transfer coefficient and friction factor correlations for the transitional flow regime in rib roughened rectangular ducts. *International J. of Heat and Mass Transfer*. 1999, 42(9), 1597-1615.
- [19] Momin A-M.E., Saini J.S., Solanki S.C. Heat transfer and friction in solar air heater duct with V-shaped rib roughness on absorber plate. *International J. of Heat and Mass Transfer*. 2002, 45(16), 3383-3396.
- [20] Muluwork K.B., Saini J.S., Solanki S.C. Studies on discrete rib roughened solar air heaters. *Proceedings of National Solar Energy Convention*. Roorkee, India, 1998.
- [21] Layek A., Saini J.S., Solanki S.C. Heat transfer and friction characteristics for artificially roughened ducts with compound turbulators. *International J. of Heat and Mass Transfer*. 2007, 50(23-24), 4845-4854.
- [22] Mittal M.K., Varun, Saini R.P., Singal S.K. Effective efficiency of solar air heaters having different types of roughness on absorber plate. *Energy*. 2007, 32(5), 739-745.
- [23] Petela R. Exergy of undiluted thermal radiation. *Solar Energy*. 2003, 74(6), 469-488



Mridul Sharma has been graduated in Mechanical Engineering in 2007 and completed M.Tech in 2009 from NIT Hamirpur (India) in Thermal specialization with Computational Fluid Dynamics and Heat Transfer. Currently he is working as a Lecturer in Department of Mechanical Engineering at National Institute of Technology, Hamirpur, India. His area of interest is Heat Transfer, Solar Energy and Non-conventional Energy Sources.

E-mail address: mridul.sharma08@gmail.com



Varun has been graduated in Mechanical Engineering in 2002 and after that completed his M.Tech in Alternate Hydro Energy Systems in 2004 from IIT Roorkee (India). He is presently working as a Lecturer in Department of Mechanical Engineering at National Institute of Technology, Hamirpur, India. His area of interest is Solar Air Heater, Life Cycle Assessment and Heat Transfer. He has been published more than 20 papers in International / National Journals.

E-mail address: varun7go@gmail.com

